the user's diffractometer but, with line-profile-fitting programs now available, the $K\alpha_2$ component can be modelled precisely along with the $K\alpha_1$.

It is possible to isolate the $K\alpha_1$ line when using a high-quality incident-beam focusing monochromator as described in Subsection 2.3.1.2, Fig. 2.3.1.12(*b*), but there may be a loss of intensity. The source size must be narrow and the focal length long enough to separate the components.

2.3.3.3. *Use of peak or centroid for angle definition*

The most obvious and commonly used measure of the reflection angle of a profile is the position of maximum intensities (Fig. 2.3.3.3). The midpoints of chords at various heights have often been used but their values vary with the profile asymmetry. Another method is to connect the midpoints of chords near the top of the profile and extrapolate to the peak. The computer methods using derivatives are the most accurate and fastest as described in Subsection 2.3.3.7.

A more fundamental measure that uses the entire intensity distribution is the centre of gravity (or centroid) defined as

$$\langle 2\theta \rangle = \int 2\theta I(2\theta)\,\mathrm{d}(2\theta) \Big/ \int I(2\theta)\,\mathrm{d}(2\theta). \qquad (2.3.3.5)$$

The variance (mean-square deviation of the mean) is defined as

$$W_{2\theta} = \langle (2\theta - \langle 2\theta \rangle)^2 \rangle = \int (2\theta - \langle 2\theta \rangle)^2 I(2\theta)\,\mathrm{d}(2\theta) \Big/ \int I(2\theta)\,\mathrm{d}(2\theta). \qquad (2.3.3.6)$$

The use of the centroid and variance has two important advantages: (1) most of the aberrations (§2.3.1.1.6) were derived in terms of the centroid and variance; and (2) they are additive, making it easy to determine the composite effect of a number of aberrations. Mathematically, the integration extends from $-\infty$ to $+\infty$ but the aberrations have a finite range. However, the practical use of these measures causes some difficulty. If the profile shapes are Lorentzian, the tails decay slowly. A very wide range would be required to reach points where the signal could no longer be separated from the background and the profiles must be truncated for the calculation. Truncation limits that have been used are 90% ordinate heights of $K\alpha_1$ (Ladell, Parrish & Taylor, 1959), and equal 2θ or λ limits from the centroid (Taylor, Mack & Parrish, 1964; Langford, 1982). The limits such as $2\theta_1$ and $2\theta_2$ in Fig. 2.3.3.3 must be carefully chosen to avoid errors and this involves the correct determination of the background level. It is not practical to use centroids for overlapping peak clusters unless the profile fitting can accurately resolve the individuals with their correct positions and intensities. Their use has, therefore, been confined to simple patterns with small unit cells in which the profiles were well separated.

The difference between the angle derived from the peak and the centroid depends on the asymmetry of the profile, which in turn varies with the $K\alpha$-doublet separation and the aberration broadening. Tournarie (1958) found that the centre of a horizontal chord at 60.6% of the $K\alpha_1$ peak height corresponds well to the centroid of that line in fairly well resolved doublets. The number, of course, depends on the profile shape. There is also the basic problem that most of the X-ray wavelengths were probably determined from the spectral peaks and, if the centroids are measured for the powder pattern, the Bragg equation becomes nonlinear in the sense that the 1:1 correspondence between λ and $\sin\theta$ is lost.

2.3.3.4. *Rate-meter/strip-chart recording*

Formerly, the most common method of obtaining diffractometer data was by using a rate-meter and strip-chart recorder with the paper moving synchronously with the constant angular velocity of the scan. This simple analogue method is still used and a large fraction of the JCPDS (ICDD) file prior to about 1982 was obtained in this way.

The method has several limitations: the data are not in the digital form required for computers, and are distorted; manual measurement of the chart takes a long time and has low accuracy. The output of the strip chart lags behind the input by an amount determined by the product of the scanning speed and the time constant of the rate-meter, including the speed of the recorder pen. The peak height is decreased and shifted in the direction of the scan causing asymmetric broadening with loss of resolution. The profile shape, $K\alpha$-doublet separation, and scan direction also contribute to distortion. When the product of the scan speed and time constant have the same value, the profile shapes are the same even though the total count is determined by the scan speed, Figs. 2.3.3.4(*a*) and (*b*). If the product is large, the distortion is severe (*c*), and very weak peaks may be lost.

2.3.3.5. *Computer-controlled automation*

Most diffractomers are now sold with computer automation. Older instruments can be easily upgraded by adding a stepping motor to the gear-drive shaft. A large variety of computers and programs is available, and it is not easy to make the best selection. Continuing improvements in computer technology have been made to handle expanded programs with increased speed and storage capabilities. The collected data are displayed on a VDU screen and/or computer printer and stored on hard disk or diskette for later use and analysis. Microprocessors are often used to select the X-ray-generator operating conditions, shutter control, specimen change, and similar tasks that were formerly performed manually. Aside from the elimination of much of the manual labour, automation provides far better control of the data-collection and data-reduction procedures. However, computers do not preclude the necessity of precise alignment and calibration. Smith (1989) has written a detailed description of computer analysis for phase identification and also includes related programs and their sources.

Personal computers are widely used for powder-diffraction automation and a typical arrangement is shown in Fig. 2.3.3.5(*a*). The automation may provide for step scanning,

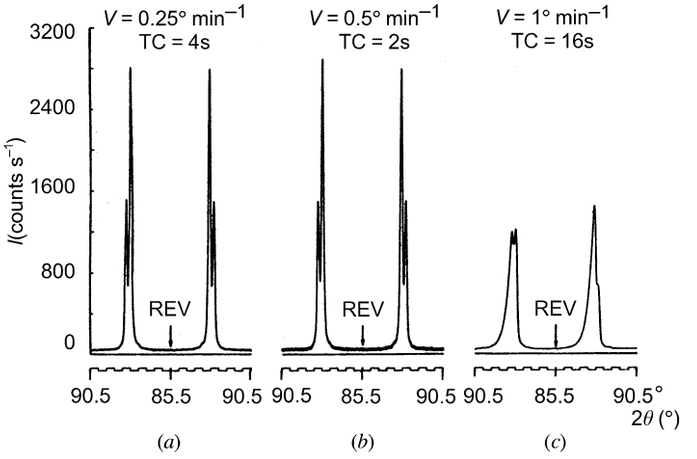

Fig. 2.3.3.4. Rate-meter strip-chart recordings. REV: scan direction reversed. Scan speed and time constant shown at top.

continuous scanning with read-out on the fly, or slewing to selected angles to read particular points. Step scanning is the method most frequently used. It is essential that absolute registration and step tracking be reliably maintained for all experimental conditions.

The step size or angular increment $\Delta 2\theta$ and count time t at each step, and the beginning and ending angles are selectable. For a given total time available for the experiment, it usually makes no difference in the counting statistical accuracy if a combination of small or large $\Delta 2\theta$ and t (within reasonable limits) is used. A minimal number of steps of the order of $\Delta 2\theta \simeq 0.1$ to 0.2 FWHM is required for profile fitting isolated peaks. It is clear that the greater the number of steps, the better the definition of the profile shape. The step size becomes important when using profile fitting to resolve patterns containing overlapped reflections and to detect closely spaced overlaps from the width and small changes in slopes of the profiles. A preliminary fast run to determine the nature of the pattern may be made to select the best run conditions for the final pattern. Will *et al.* (1988) recorded a quartz pattern with 1.28 Å synchrotron X-rays and 0.01° steps to test the step-size role. The profile fitting was done using all points and repeated with the omission of every second, third, and fourth point corresponding to $\Delta 2\theta = 0.02$, 0.03 and 0.04°. The R(Bragg) values were virtually the same (except for 0.04° where it increased), indicating the experimental time could have been reduced by a factor of three with little loss of precision; see also Hill & Madsen (1984). Patterns with more overlapping would require smaller steps. Ideally, the steps could be larger in the background but this also requires a prior knowledge of the pattern and special programming.

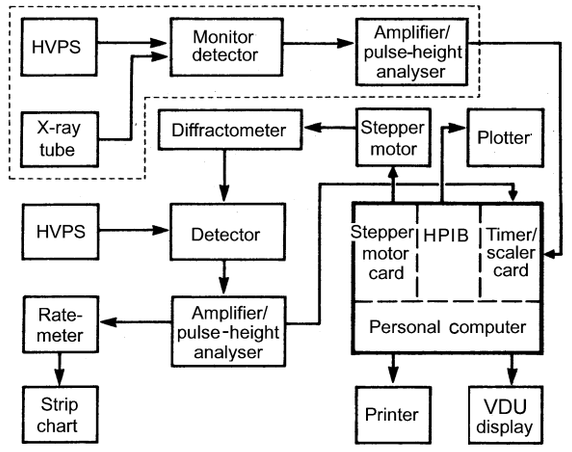

(*a*)

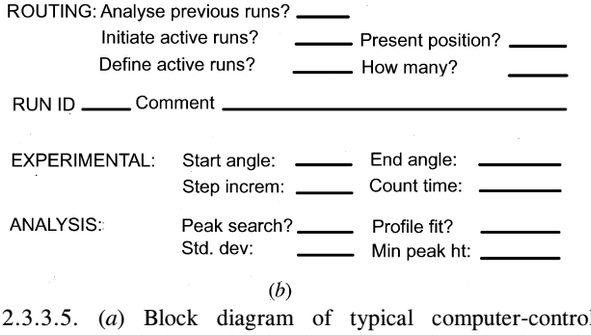

(*b*)

Fig. 2.3.3.5. (*a*) Block diagram of typical computer-controlled diffractometer and electronic circuits. The monitor circuit enclosed by the dashed line is optional. HPIB is the interface bus. (*b*) A full-screen menu with some typical entries.

A typical VDU screen menu for diffractometer-operation control is shown in Fig. 2.3.3.5(*b*). A number of runs can be defined with the same or different experimental parameters to run consecutively. The run log number, date, and time are usually automatically entered and together with the comment and parameters are carried forward and recorded on the print-outs and graphics to make certain the runs are completely identified. The menu is designed to prompt the operator to enter all the required information before a run can be started. Error messages appear if omissions or entry mistakes are made. There are, of course, many variations to the one shown.

2.3.3.6. *Counting statistics*

X-ray quanta arrive at the detector at random and varying rates and hence the rules of statistics govern the accuracy of the intensity measurements. The general problems in achieving maximum accuracy in minimum time and in assessing the accuracy are described in books on mathematical statistics. Chapter 7.5 reviews the pertinent theory; see also Wilson (1980). In this section, only the fixed-time method is described because the fixed-count method takes too long for most practical applications.

Let $\bar{N}$ be the average of N, the number of counts in a given time t, over a very large number of determinations. The spread is given by a Poisson probability distribution (if $\bar{N}$ is large) with standard deviation

$$\sigma = \bar{N}^{1/2}. \qquad (2.3.3.7)$$

Any individual determination of N or the corresponding counting rate n $(= N/t)$ will be subject to a proportionate error ε which is also a function of the confidence level, *i.e.* the probability that the result deviates less than a certain percentage from the true value. If Q is the constant determined by the confidence level, then

$$\varepsilon = Q/N^{1/2}, \qquad (2.3.3.8)$$

where $Q = 0.67$ for the probable relative error ε_{50} (50% confidence level) and $Q = 1.64$ and 2.58 for the 90 and 99% confidence levels (ε_{90}, ε_{99}), respectively. For a 1% error, $N = 4500$, 27 000, 67 000 for ε_{50}, ε_{90}, ε_{99}, respectively. Fig. 2.3.3.6 shows various percentage errors as a function of N for several confidence levels.

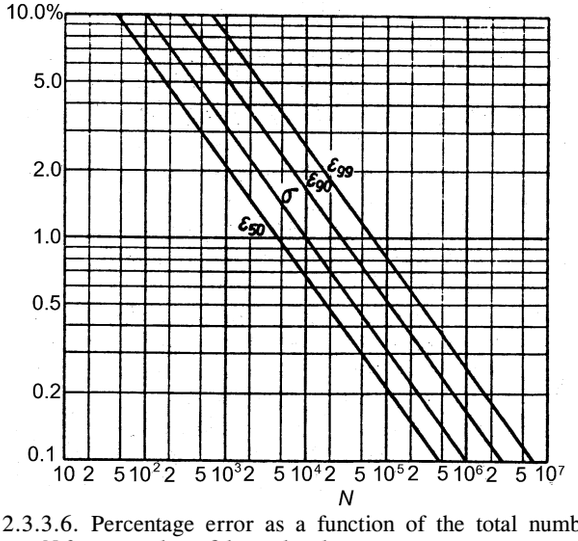

Fig. 2.3.3.6. Percentage error as a function of the total number of counts N for several confidence levels.

references